Acta Crystallographica Section D
Biological Crystallography
ISSN 0907-4449

Structures of the oxidized and reduced forms of nitrite reductase from *Rhodobacter sphaeroides* 2.4.3 at high pH: changes in the interactions of the type 2 copper

Frida Jacobson,[a] Hongwei Guo,[b] Kenneth Olesen,[c] Mats Ökvist,[d] Richard Neutze[a]* and Lennart Sjölin[e]*

[a]Department of Chemistry and Bioscience, Chalmers University, Box 462, SE-405 30 Göteborg, Sweden, [b]Structural Chemistry Laboratory, AstraZeneca R&D Mölndal, SE-431 83 Mölndal, Sweden, [c]Department of Medical Biochemistry, Göteborg University, Box 440, SE-405 30 Göteborg, Sweden, [d]Center for Structural Biology and Department of Chemistry and Biophysics, Göteborg University, Box 462, SE-405 30 Göteborg, Sweden, and [e]Center for Structural Biology and Department of Inorganic Chemistry, Göteborg University, SE-412 96 Göteborg, Sweden

Correspondence e-mail: richard.neutze@chembio.chalmers.se, sjolin@chem.gu.se

Received 28 January 2005
Accepted 2 June 2005

PDB References: nitrite reductase, oxidized, 1zv2, r1zv2sf; reduced, 2a3t, r2a3tsf.

Nitrite reductase is an enzyme operating in the denitrification pathway which catalyses the conversion of nitrite (NO_2^-) to gaseous nitric oxide (NO). Here, crystal structures of the oxidized and reduced forms of the copper-containing nitrite reductase from *Rhodobacter sphaeroides* 2.4.3 are presented at 1.74 and 1.85 Å resolution, respectively. Whereas the structure of the enzyme is very similar to those of other copper-containing nitrite reductases, folding as a trimer and containing two copper sites per monomer, the structures reported here enable conformational differences between the oxidized and reduced forms of the enzyme to be identified. In the type 1 copper site, a rotational perturbation of the side chain of the copper ligand Met182 occurs upon reduction. At the type 2 copper site, a dual conformation of the catalytic residue His287 is observed in the oxidized structure but is lacking in the reduced structure, such that the interactions of the oxidized type 2 copper ion can be regarded as adopting octahedral geometry. These findings shed light on the structural mechanism of the reduction of a copper-bound nitrite to nitric oxide and water.

1. Introduction

Inorganic nitrogen, such as in nitrates and nitrites, is introduced into the biosphere by the biological fixation of dinitrogen and is removed from the biosphere through denitrification. In dissimilatory denitrification (Zumft, 1997), nitrate is used as an alternative electron acceptor during respiration when oxygen is scarce. It is a vital part of the bioenergetic engine of the cell in denitrifying bacteria, which occupy a wide range of natural habitats. Nitrate is reduced in stages through a series of redox proteins to NO_2^-, $NO_{(g)}$, $N_2O_{(g)}$ and finally to $N_{2(g)}$. The nitrogen cycle has received much attention in recent years owing to the fact that several substrates and products of the pathway are known to be environmental pollutants (Suzuki *et al.*, 1999). Furthermore, the process is the only means by which gaseous nitrogen can be returned to the atmosphere.

Nitrite is the toxic product of the reduction of nitrate and its reduction to NO is considered to be a key step in the dissimilatory denitrification pathway as this step leads to a gaseous intermediate,

$$NO_2^- + 2H^+ + e^- \longrightarrow NO_{(g)} + H_2O. \quad (1)$$

At high levels, $NO_{(g)}$ is toxic to the host and therefore it is of great importance for the bacteria to regulate the concentration of NO. This regulation is performed by the controlled

expression of two enzymes: nitrite reductase (NiR), which produces NO, and NO reductase, which reduces NO to N_2O.

There are two main categories of NiRs: those that are haem-containing (cd1-NiRs; Fülöp *et al.*, 1995; Nurizzo *et al.*, 1997) and those that are copper-containing (Cu-NiRs; Inoue *et al.*, 1998; Adman *et al.*, 1995; Dodd *et al.*, 1997, 1998; Kukimoto *et al.*, 1994). All studied copper-containing NiRs contain both type 1 and type 2 copper centres (six Cu atoms per enzyme). The type 1 Cu centre is coordinated by two histidines, a cysteine and a methionine and the type 2 Cu centre is co-ordinated by three histidines and a water molecule (Adman *et al.*, 1995). Nitrite binds at the type 2 copper site (Howes *et al.*, 1994) and upon an electron being delivered to this site *via* the type 1 Cu site (Kukimoto *et al.*, 1994; Libby & Averill, 1992; Abraham *et al.*, 1993) the nitrite is reduced to NO and water. Before the produced NO leaves the type 2 Cu site, it is bound to the copper ion in a side-on copper-nitrosyl intermediate (Tocheva *et al.*, 2004). It is the type 1 copper site which absorbs in the visible spectrum, giving all NiRs their colour. Based upon their colour, the Cu-NiRs can be further classified as either green or blue NiRs (Suzuki *et al.*, 1999). As with other cupredoxins, such as azurin and plastocyanin (Sykes, 1991), the oxidized forms of Cu-NiRs display an intensely blue absorption peak around 600 nm. In addition, the green nitrite reductases have a second yellow absorption peak around 460 nm.

The first Cu-NiR X-ray structure was reported from *Achromobacter cycloclastes* (AcNiR; PDB code 2nrd; Adman *et al.*, 1995). This study revealed that the functional enzyme folded as an active homotrimer, with two well conserved histidine residues entering from an adjacent monomer to complete the type 2 copper active site of nitrite reduction. Each monomer (~40 kDa) was further divided into two Greek-key β-barrel domains, the type 1 Cu atom being located inside one such domain, just beneath the protein surface, and the type 2 Cu atom being located between two domains, buried at the interface between two monomers. This fold and active form of the enzyme has proven to be well conserved throughout the families of both the blue (Inoue *et al.*, 1998; Dodd *et al.*, 1997, 1998) and the green (Adman *et al.*, 1995; Kukimoto *et al.*, 1994) NiRs. From these structural results together with kinetic studies, it was reasoned that the type 1 Cu first accepts an electron from an upstream donor (azurin, pzeudoazurin or a cytochrome c_2) and relays this to the type 2 Cu site, where nitrite is reduced (Kukimoto *et al.*, 1994; Libby & Averill, 1992; Abraham *et al.*, 1993). These copper sites are ~12 Å apart and are directly connected through perfectly conserved cysteine and histidine residues, which are ligands to the type 1 and type 2 Cu sites, respectively.

Since these pioneering structural results, attention has focused on the detailed mechanism of nitrite reduction at the type 2 Cu, the regulation of the electron transfer from the type 1 to the type 2 Cu site, the binding of the upstream electron donor to NiR and the possible cause and functional implications of the strong yellow absorption maxima in the green NiRs (Suzuki *et al.*, 1999; Basumallick *et al.*, 2003). A mechanism in which the enzyme regulates the flow of electrons between the two Cu sites has been proposed in which electron movement from the type 1 to the type 2 Cu is believed to occur only after the binding of nitrite to the type 2 Cu (Boulanger *et al.*, 2000; Farver *et al.*, 2004). This postulation is based upon a variety of kinetic studies on specific NiR mutants (Olesen *et al.*, 1998; Strange *et al.*, 1999).

Here, we describe the X-ray structures at high resolution of both the reduced and oxidized forms of nitrite reductase from *Rhodobacter sphaeroides* 2.4.3 (RsNiR), a copper-containing green NiR with strong absorption peaks at 457 nm and 590 nm (Olesen *et al.*, 1998). This work provides the first native X-ray structures of NiR from this source and shows good agreement with other Cu-containing NiRs structures determined to date. Compared with the previously established sequence of RsNiR (Tosques *et al.*, 1997), six sequence corrections were identified from the X-ray structures of RsNiR. Structural comparisons between the oxidized and reduced forms of this enzyme showed that Met182, which provides one of two S atoms coordinating the type 1 Cu ion, has distinctly different conformations depending upon the redox state of this Cu ion. At the type 2 Cu site, a water molecule that ligates the Cu ion when the enzyme is oxidized is lost when the enzyme is reduced, as previously reported for another Cu-NiR (Murphy *et al.*, 1997). In addition, we observe (at pH 8.4) that the catalytic His287 located near the type 2 Cu adopts a dual conformation in the oxidized enzyme, but not in the reduced enzyme. This finding suggests that it is possible to regard the interactions of this metal site as having a distorted octahedral geometry rather than the distorted tetrahedral geometry more frequently discussed for copper proteins. The potential significance of this octahedral geometry during enzyme catalysis is discussed and the interactions of the oxidized type 2 Cu site are compared with those of the reduced site.

2. Materials and methods

Wild-type RsNiR was expressed in *Escherichia coli*: 6 × 1 l cultures were inoculated 1:100 with overnight pre-cultures. $CuSO_4$ was added to a final concentration of 0.6 m*M*. All cultures were induced with IPTG at OD_{600} = 0.5 and the cells were harvested 3 h later. The cells were resuspended in a small amount of 50 m*M* phosphate buffer pH 7.2 and broken by passing through an X-Press. Cell debris was removed by ultracentrifugation for 40 min at 35 000 rev min^{-1} (Ti-45 rotor) and the supernatant was placed in a heating block for 10 min at 343 K. After 45 min ultracentrifugation at 40 000 rev min^{-1} (Ti-45 rotor), $CuSO_4$ was added to the now clear supernatant to a final concentration of 1 m*M*, turning the solution green. The protein solution was loaded onto an anion-exchange column (Q Sepharose Fast Flow, Pharmacia) and washed with 50 m*M* phosphate buffer pH 7.2. RsNiR was eluted with a salt gradient from 50 to 500 m*M* NaCl and the green fractions were pooled. Finally, the protein solution was dialysed against 10 m*M* Bis-Tris pH 7.0 in a dialysis tube with 50 kDa cutoff to remove the inactive monomeric form of the protein.

Vapour diffusion was used for crystallization, with the drop containing 2 µl protein and 2 µl reservoir solution. The protein concentration was 0.1 m*M* and the reduced protein sample was reduced prior to crystallization, with a final concentration of 20 m*M* sodium ascorbate. The reservoir solutions contained 0.15–0.22 *M* $MgCl_2$, 19–23% PEG 4000 and 0.1 *M* Tris pH 8.4. The reservoirs of the reduced crystal setups also contained 20 m*M* sodium ascorbate. After setup at room temperature, the blue–green oxidized crystals appeared within a few days and were frozen after two weeks. A cryoprotectant with 10% of the PEG 4000 replaced by PEG 400 was used. The dimensions of the oxidized crystal were approximately 0.2 × 0.2 × 0.2 mm. The colourless reduced crystal appeared a few days later than the oxidized crystal and its dimensions were approximately 0.05 × 0.05 × 0.05 mm. The reduced crystal was still colourless when frozen.

Data were collected at the synchrotron facility I 7-11 at MaxLab II in Lund, Sweden. The detector used was a MAR Research 165 mm CCD detector and the temperature was set to 100 K. The radiation wavelengths were 1.017 and 1.007 Å for the reduced and oxidized data sets, respectively. *DENZO* was used for processing the data and *SCALEPACK* was used for scaling and merging (Otwinowski & Minor, 1997). Data from both data sets were processed in space group *R*3 with one monomer per asymmetric unit and after scaling the data sets for oxidized and reduced RsNiR were cut at 1.74 and 1.85 Å resolution, respectively. *AMoRe* (Navaza, 1994) was used for molecular replacement using NiR from *A. cycloclastes* as a search model (PDB code 1nif; 65% sequence identity with RsNiR). The molecular-replacement solution which was used resulted in *R* factors of 44%. After one round of rigid-body refinement in *CCP*4, simulated annealing was carried out in *CNS* (Brünger *et al.*, 1998). Rigid-body refinement and simulated annealing were performed without adding Cu atoms or solvent molecules, which were instead added utilizing the *ARP*/*wARP* (Lamzin & Wilson, 1993) function in *REFMAC*5. Both coppers were first added as water molecules but recognized as Cu atoms owing to their low *B* factors. When analysing the solvent molecules, three additional heavy atoms were found in the structure and were assigned as magnesiums owing to coordination properties and metal–ligand distances. Model building was performed in *O* (Jones *et al.*, 1991) and omit maps were calculated in *CNS*. For a few amino-acid side chains, dual conformation was modelled. Both structures were analysed using *PROCHECK* (Laskowski *et al.*, 1993) and the final properties of the models are presented in Table 1. The geometric properties of the two Cu sites are presented in Table 2.

Table 1
Data-collection and refinement parameters for oxidized and reduced RsNiR.

Values in parentheses show data for the last resolution shell (1.81–1.74 Å for oxidized RsNiR and 1.92–1.85 Å for reduced RsNiR).

	Oxidized RsNiR	Reduced RsNiR
Radiation wavelength (Å)	1.007	1.017
Temperature (K)	100	100
Resolution (Å)	1.74	1.85
Space group	*R*3	*R*3
Unit-cell parameters (Å, °)	$a = b = 72.4$, $c = 147.5$, $\alpha = \beta = 90$, $\gamma = 120$	$a = b = 72.4$, $c = 148.1$, $\alpha = \beta = 90$, $\gamma = 120$
Monomers per asymmetric unit	1	1
No. of observed reflections	79426	144592
No. of unique reflections	29034 (2973)	24723 (2472)
Reflections in test set (%)	5.0	5.0
Completeness (%)	98.6 (100)	100 (100)
Redundancy	2.9 (2.7)	5.9 (5.8)
$I/\sigma(I)$	9.7 (2.9)	8.5 (4.1)
R_{merge} (%)	6.5 (34)	7.9 (49)
No. of residues	328	328
No. of atoms (non-H)	2792	2723
No. of solvent molecules	292	236
No. of Mg^{2+} ions	3	3
No. of Cu^{2+}/Cu^{+} ions	2	2
R_{work} (%)	15.2	14.4
R_{free} (%)	19.1	17.6
R.m.s.d. bond lengths (Å)	0.013	0.016
R.m.s.d. bond angles (°)	1.5	1.5
Average *B* factor, protein	15.0	21.3
Average *B* factor, waters	24.4	31.8
Ramachandran plot		
Residues in most favoured regions (%)	90.2	91.0
Residues in additionally allowed regions (%)	8.2	9.0

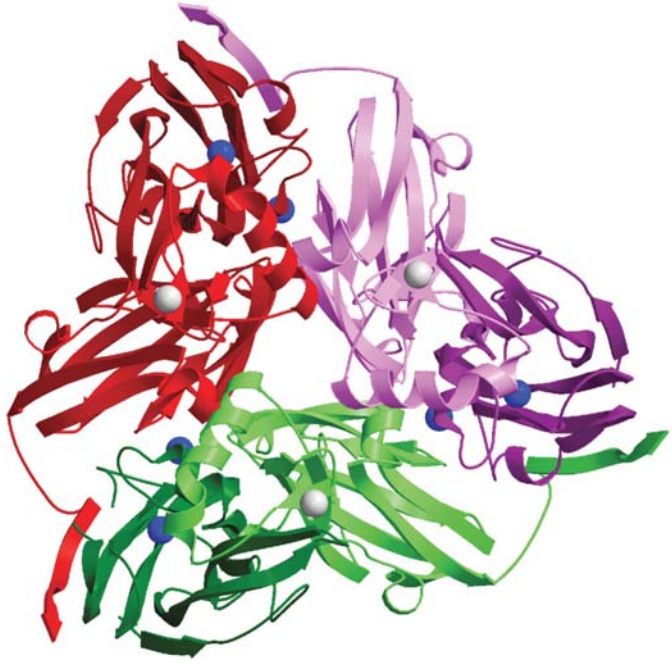

Figure 1
Overview of the trimeric form of RsNiR. Copper ions are shown in blue and the magnesium ions that stabilize surface loops (see text for details) are shown in grey. (This figure was produced with *MOLSCRIPT*.)

3. Results and discussion

Diffracting crystals of both the oxidized and reduced forms of RsNiR were grown at pH 8.3–8.4 and diffraction data were refined to 1.74 and 1.85 Å, respectively. As with all other Cu-containing NiRs investigated to date, the crystals form from active homotrimers which, together with copper cofactors and the three magnesium ions that stabilize three corresponding surface loops, are shown in Fig. 1. The r.m.s.d.s of the backbone C^{α} atoms of this structure relative to other Cu-NiR structures are presented in Table 3. All differences are less than 0.8 Å and the mean difference relative to the blue NiRs is 0.703 Å compared with a mean difference of 0.565 Å for the green NiRs. Sequencing errors at Asp230, Asn281, Ser319, His351, Val367 and Ala368 were identified in both structures (see supplementary figure[1]) compared with the previously published sequence (Tosques *et al.*, 1997). These residues lie neither within the Cu site nor along the hypothetical electron-transfer pathway and are not believed to be critical to function. No electron density was observed for residues 1–43 at the N-terminus; the first 38 residues are presumably cleaved prior to folding (Olesen *et al.*, 1998). These additional N-terminal residues lead to a non-standard numbering for RsNiR, so that the first amino acid of the active protein is numbered 39. A hydrophobic patch on the surface, ∼6 Å from the type 1 copper, is observed as previously reported for numerous blue copper proteins (Inoue *et al.*, 1998; Adman *et al.*, 1995; Dodd *et al.*, 1997, 1998; Kukimoto *et al.*, 1994) and provides a docking site for the upstream electron donor. Just beneath this hydrophobic surface lies the copper ligand His177 that presumably delivers an electron to the copper in the type 1 site. Three magnesium ions were identified within the structure of one monomer and one was seen to stabilize the protruding loop 218–227 by ligating Asp220, Thr224 and four water molecules. This magnesium ion (shown in Fig. 1) mediates crystal packing by forming a bridge from residues 220 and 224 to residue 205 of another molecule *via* hydrogen bonding to one of its water ligands. The other two magnesium ions coordinate solvent ligands only and are not shown in Fig. 1.

There has been much discussion about the origin of the spectral differences between green and blue NiRs (Inoue *et al.*, 1998; Dodd *et al.*, 1997, 1998; Olesen *et al.*, 1998; Pierloot *et al.*, 1998; Adman *et al.*, 1995; Wijma *et al.*, 2003). While a consensus picture has emerged in which the blue peak at 600 nm is believed to derive from π back-bonding between Cys167 and the type 1 Cu (Fee, 1975), there has been considerable debate as to the origin of the 460 nm absorption peak in the green NiRs that is suppressed in the blue NiRs. Many suggestions have been offered, including the distance of the coordinating S atom of the methionine ligand to the type 1 Cu (Olesen *et al.*, 1998; Basumallick *et al.*, 2003), the displacement of the copper ion from the His—His—Cys ligand plane (Dodd *et al.*, 1997, 1998), the angle between the S—Cu—S and the N—Cu—N planes of the Cu-ligating S and N atoms (Figs. 2 and 3; Pierloot *et al.*, 1998), the influence on the methionine ligand on close-lying amino acids (Inoue *et al.*, 1998) and the electronic environment immediately surrounding the Cu ion (Basumallick *et al.*, 2003; Wijma *et al.*, 2003). Recently, Basumallick and coworkers performed a thorough study on the electronic structures of type 1 Cu centres using NiR from *A. cycloclastes* and M182T RsNiR as two of the models (Basumallick *et al.*, 2003). The mutant M182T has a threonine in place of the type 1 Cu methionine ligand, which converts the enzyme colour from green to blue owing to changes in the electronic environment of the type 1 Cu centre (Olesen *et al.*, 1998). The distance of the Met182 S atom from the type 1 Cu is 2.46 Å in our oxidized structure of RsNiR and the same distance for the other structurally determined Cu-NiRs is 2.59 Å in the two green NiRs, and 2.62 and 2.59 Å in the blue NiRs.

Table 2
Geometric properties for the copper sites in oxidized and reduced RsNiR.

	Oxidized RsNiR	Reduced RsNiR
Distances in type 1 Cu site (Å)		
Cu—S (Met182)	2.46	2.43
Cu—S (Cys167)	2.20	2.23
Cu—N (His126	2.03	2.18
Cu—N (His177)	2.03	2.10
Distances in type 2 Cu site (Å)		
Cu—NE (His131)	2.01	2.04
Cu—NE (His166)	2.05	2.03
Cu—NE (His338)	2.15	2.11
Cu—water306	1.96	—
Cu—OD2 (Asp129)	3.34	3.50
Cu—NE (His287)		3.83
Close conformation	2.64	—
Distant conformation	3.81	—

There is no obvious correlation between the distance from the methionine S atom to the type 1 copper and the protein colour; therefore, attention has focused on the angle θ between the plane formed by the coordinating N—Cu—N atoms of His126 and His177 and the plane formed by the coordinating S—Cu—S atoms of Cys167 and Met182 with the

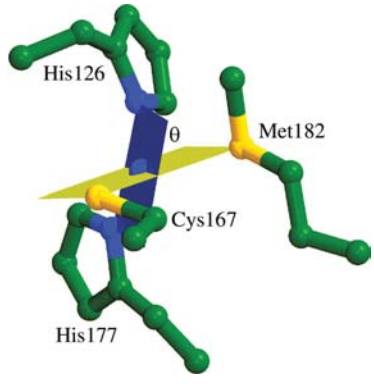

Figure 2
Representation of the acute angle between the S—Cu—S plane (yellow) and the N—Cu—N plane (blue) of the type 1 Cu site from RsNiR. In the text this angle is referred to as θ. (This figure was produced with *MOLSCRIPT*.)

[1] Supplementary material has been deposited in the IUCr electronic archive (Reference: HV5033). Services for accessing these data are described at the back of the journal.

Table 3
R.m.s.d.s (Å) between Cu-NiR structures from different sources.

Ac, *Achromobacter cycloclastes*; Ax, *Alcaligenes xylosoxidans*; Af, *Alcaligenes faecalis*.

	AcNiR†	AfNiR†	AxNiR‡ (GIFU1051§)	AxNiR‡	RsNiR† (reduced)
PDB code	2nrd	1as7	1bq5	1ndt	2a3t
RsNiR† (oxidized)	0.603	0.527	0.682	0.725	0.107

† Green NiRs. ‡ Blue NiRs. § GIFU1051 is a specific strain of *A. xylosoxidans*.

central Cu atom (Fig. 2). Both theoretical and experimental arguments (Pierloot *et al.*, 1998; Basumallick *et al.*, 2003) show that a high value of θ (close to 90°) correlates with a high value in the ratio of the two absorption peaks, A_{600}/A_{460}. Conversely, a lower value of θ leads to a correspondingly lower value of this ratio. For oxidized RsNiR, $\theta = 67^\circ$ and $A_{600}/A_{460} \simeq 1$ (Fig. 3). This value for θ as measured from the refined X-ray structure correlates almost exactly with that expected from the empirical curve of the ratio of these two spectral absorption peaks in other Cu proteins (Fig. 3; Wijma *et al.*, 2003). This further supports the suggestion that this angle determines the spectral characteristics of the Cu-containing NiRs (Basumallick *et al.*, 2003; Ryde *et al.*, 2000).

Structural comparisons between the oxidized and reduced structures of *Alcaligenes faecalis* NiR (AfNiR) have previously been reported (Murphy *et al.*, 1997). In these studies, it was observed that a water molecule in the oxidized form of the enzyme, which was found to be coordinating the type 2 Cu site, was lost upon reduction of the enzyme, but no quantified structural changes were reported for the type 1 Cu site. In contrast with these earlier studies, here we reduced the enzyme prior to crystallization rather than reducing crystals of the oxidized enzyme (Murphy *et al.*, 1997). A motivation for this change in methodology derives from studies of the haem-containing cytochrome cd_1 NiR from *Pseudomonas aeruginosa*, for which very large-scale structural differences were observed in the X-ray structures of the reduced enzyme dependent upon whether the enzyme was reduced prior to or following crystallization (Sjogren & Hajdu, 2001). Nevertheless, for the Cu-containing RsNiR no large-scale conformational changes emerged as a consequence of reduction of the enzyme prior to crystallization: both the oxidized and reduced RsNiR have very similar structures, with the r.m.s.d. value being 0.25 Å when superimposing all peptide atoms and 0.11 Å when superimposing only C^α atoms. Two residues were modelled as having dual conformation in both structures: Glu72 and Met93. Away from the active site, the residues that have well defined conformations that differ between the two structures are Val52, Ile78, Glu113, Val202, Val207 and Arg308. These residues are unlikely to affect the function of the protein and the differences in conformation are most likely to be artefacts of the different crystallization conditions, *i.e.* the addition of ascorbate for the reduced crystals. However, in addition to the above differences several structural details near the Cu active sites which have not been described previously can be reported at high resolution.

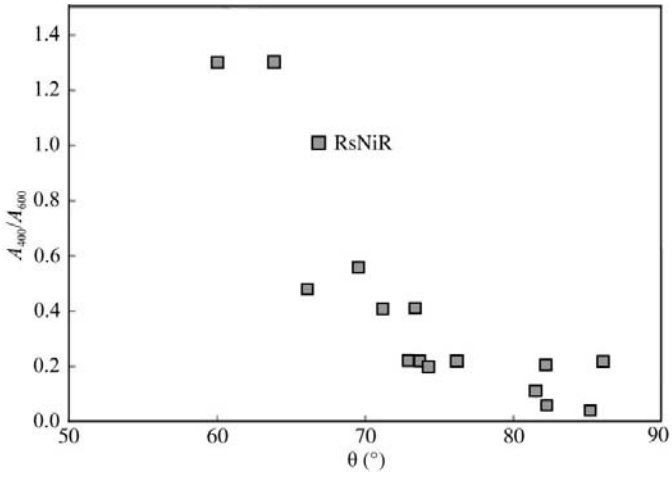

Figure 3
The acute angle θ between the two planes $S_{Met}-Cu-S_{Cys}$ and $N_{His}-Cu-N_{His}$ of the type 1 Cu centre in relation to the absorption peak ratio A_{460}/A_{600} for a number of Cu proteins (Wijma *et al.*, 2003). (This figure was prepared with data from from Wijma *et al.*, 2003, manipulated in *CorelDraw*.)

In Fig. 4 the structural models and electron density for Met182 in the oxidized (Fig. 4*a*) and reduced (Fig. 4*b*) forms of RsNiR are shown in the immediate vicinity of the type 1 Cu site. In both the oxidized and the reduced form the type 1 Cu site has a distorted tetrahedral geometry and the coordinating residues to this Cu are His126 N^δ, His177 N^δ, Cys167 S^γ and Met182 S^δ. A previously unreported change in the conformation of the Cu ligand Met182 is apparent when comparing the reduced and oxidized electron densities and refined structures. Whereas the location of the S atoms is almost unchanged in the two cases, this side chain is oriented with the arrowhead formed by the $C^\gamma-S-C^\varepsilon$ atoms of Met182 pointing somewhat away from the Cu atom in the oxidized form of the enzyme, yet the same arrowhead is directed significantly more towards the Cu metal atom in the reduced form. This change can be described in polar coordinates with the centre at the S-atom position (Chakrabarti, 1989). The φ angle is the angle between the bisector of the angle C—S—C of Met182 and the line from its S atom to the projection of Cu in the C—S—C plane. The angle ψ is the angle between the normal to the plane C—S—C and the line S—Cu. These angles increase by 10 and 17°, respectively, as the copper changes from the oxidized state to the reduced state, but the S—Cu distance remains constant (Table 2). The acute angle C—S—C of the Met182 side chain also differs slightly between the two states, changing from 94° in the oxidized copper site to 102° in the reduced form.

The observed change in the conformation of the type 1 Cu ligand (Fig. 4) presumably follows from the change in the oxidation state of the copper: the additional electron in the reduced copper ion affects the bonding orbitals between the Cu atom and the Met182 S atom, leading to a difference in the geometry of the Met182 side chain. With respect to the copper, the primary difference between the two conformations is that (from geometric considerations) the interaction of the copper ion with the two unpaired sp^3 orbitals of the Met182 S atom is

Table 4
Angles (°) for the pseudo-octahedral type 2 copper site in oxidized RsNiR.

	Asp129 O	His131 N	His166 N	His287 N†	His338 N	Wat306
Asp129 O	—					
His131 N	98	—				
His166 N	74	96	—			
His287 N†	89	91	162	—		
His338 N	161	102	104	90	—	
Wat306	68	162	90	78	93	—

† Close conformation.

enhanced in the reduced form of the enzyme. It could be argued that this leads to chemically distinct environments for the Cu centre in the oxidized and reduced conformations, so that changes in the Cu^{+}/Cu^{2+} mid-point potential may arise. Hasnain and coworkers suggested that certain structural events in the reaction lead to specific and coordinated changes in the midpoint potentials of the two Cu centres, so that the flow of electrons between the two coppers is 'gated' by key events during catalysis (Strange *et al.*, 1999). Evidence for this hypothesis derives from the intriguing observations that the binding affinity of NO_2^- to the type 2 Cu active site is lowered when this site is reduced and the functionally related implication is that the type 2 Cu is not reduced by the type 1 Cu until NO_2^- is bound (Murphy *et al.*, 1997; Basumallick *et al.*, 2003). Hasnain and coworkers therefore argued that the binding of NO_2^- significantly perturbs the Cu^{+}/Cu^{2+} midpoint potentials of the two Cu sites owing to the enhanced electron-extracting properties of nitrite, to the point that the type 2 site spontaneously accepts an electron from the type 1 centre only after NO_2^- is bound (Olesen *et al.*, 1998; Strange *et al.*, 1999; Basumallick *et al.*, 2003). From the observations presented here, it is plausible that the change in conformation of Met182 from that of the oxidized form (Fig. 4*a*), where the type 1 centre accepts an electron from an upstream donor, to that of the reduced form (Fig. 4*b*), where the type 1 centre donates an electron to the type 2 centre, lowers the midpoint potential of the type 1 Cu redox centre to aid the second electron movement. Nevertheless, while small perturbations in the interaction between the Cys167 S atom and the type 1 Cu can drastically change the reduction potential of the Cu site, the accumulated evidence suggests that the influence of Met182 is much smaller (Pierloot *et al.*, 1998). It therefore appears that the maximum effect on the redox potentials of the conformational change of Met182 observed here (Fig. 4) is likely to be relatively small and should therefore be viewed as one of several contributing factors rather than the essence of a true gating mechanism.

At the type 2 Cu site, His131 and His166 from one monomer and His338 from the neighbouring monomer interact with the copper *via* their N^{ε} atoms, forming a propeller-like shape with the Cu at the centre (Fig. 5). In the oxidized protein there is a fourth ligand, a solvent molecule (Wat306) which binds to the copper, giving the site a distorted tetrahedral geometry. Consistent with previous observations (Murphy *et al.*, 1997), in this study Wat306 is seen to be disordered upon reduction. Although the X-ray structure of the reduced form of the type 2 Cu site is in full agreement with other reported X-ray structures (Murphy *et al.*, 1997), we observe here at pH 8.4 a dual conformation (50% occupancy for each conformation) of His287 in the oxidized form of the enzyme (Fig. 5) which has not previously been described. This histidine residue, which lies near the type 2 Cu site, is functionally important for both nitrite binding and nitrite reduction (Boulanger *et al.*, 2000). It is generally considered that this histidine must be protonated in order for the enzyme to function (Abraham *et al.*, 1997).

A structure of Cu-NiR from *Alcaligenes xylosoxidans* (AxNiR) has previously been reported at high pH (pH 8.5; Ellis *et al.*, 2001). When superimposed using all C^{α} atoms, AxNiR at high pH and RsNiR show a high similarity, with an r.m.s.d. of 0.69 Å. At the type 2 Cu site the structure of AxNiR has two solvent ligands with half occupancy. Based on the distances to the copper ion, these solvent molecules were interpreted as a water molecule and a hydroxyl ion. The position of the hydroxyl ion is equal to the position seen for the ligating solvent molecule in, among others, the atomic resolution structure of AxNiR (Ellis *et al.*, 2003) and the native structure of AcNiR (Adman *et al.*, 1995), and it completes an almost perfect tetrahedral geometry together with the three histidine ligands. The other ligand position, interpreted as a water molecule, does not correspond to a tetrahedral coordination around the copper ion; it has slidden down one face of the pyramid to a position almost opposite the N^{ε} of His94 (RsNiR His131), which lies on the other side of the type 2 Cu ion. This water position is also seen in, for example, the structures of native AxNiR (GIFU 1051; Inoue *et al.*, 1998) and two AfNiR mutants (Wijma *et al.*, 2003). Comparisons between our oxidized enzyme and the structure of AxNiR at high pH show that the positions of the modelled water ligands coincide. However, while our $F_o - F_c$ map shows a positive peak at the position of the hydroxyl ion, it has not been modelled owing to a lack of electron density in the $2F_o - F_c$ omit map. The histidine in AxNiR corresponding to RsNiR His287 was not modelled with a dual conformation at pH 8.5, but flexibility in this residue is hinted at since the side-chain atom *B* factors are noticeably higher than for surrounding atoms. In a structure of the membrane-associated NiR from *Neisseria gonorrhoeae*, AniA (Boulanger & Murphy, 2002), nitrite was soaked into the structure at a crystallization pH of 10.5. From a comparison of the active site and its neighbourhood in AniA and RsNiR, it was found that the hydrogen-bonding pattern and some surrounding amino acids are different. Since movement in the catalytic histidine residue is dictated by these factors, differences in them may well lead to a histidine movement that allows nitrite binding in AniA. The many small differences found are not surprising, since AniA is the soluble domain of a major anaerobically induced outer membrane protein, in contrast to other CuNiRs.

In the oxidized RsNiR structure, the dual conformation of His287 (Fig. 5) most likely arises from the high pH (of 8.4) of the crystallization experiment. The pK_a of a histidine in solution is approximately 6 and so the His287 residues should

be deprotonated at pH 8.4. Since pK_a values may be higher within a protein owing to a more hydrophobic environment, a significant fraction of the His287 residues are likely to be protonated at this pH. We suggest that the most probable interpretation of these two conformations is therefore that in the conformation with His287 most distant from the copper its imidazole ring is protonated (*i.e.* positively charged) and can therefore serve as a hydrogen-bond donor to the bridging water (Wat39), keeping the residue in position. This argument is supported by the fact that it is this conformation of His287 which is observed in other NiR structures (Adman *et al.*, 1995; Dodd *et al.*, 1997, 1998; Inoue *et al.*, 1998; Kukimoto *et al.*, 1994), the majority of which have been crystallized at lower pH. From this argument it follows that the second conformation, which has the imidazole ring deprotonated (*i.e.* neutral in charge), is unable to form the hydrogen bond to the bridging water. Together with reduced electrostatic repulsion between the copper ion and the His287 N^{ε} atom, this allows the side chain to align closer to the copper ion and the refined crystallographic structure shows that the N^{ε} atom in His287 interacts with the Cu atom at a distance of 2.6 Å.

When crystals of AfNiR were soaked in nitrite, nitrite was observed to ligate the type 2 copper ion in a bidentate fashion, with the two O atoms providing Cu ligands (Murphy *et al.*, 1997) (Fig. 6), rather than binding with the central N atom as a ligand as was anticipated. This binding property of nitrite to the Cu ion means that the type 2 Cu ion has five ligands in that

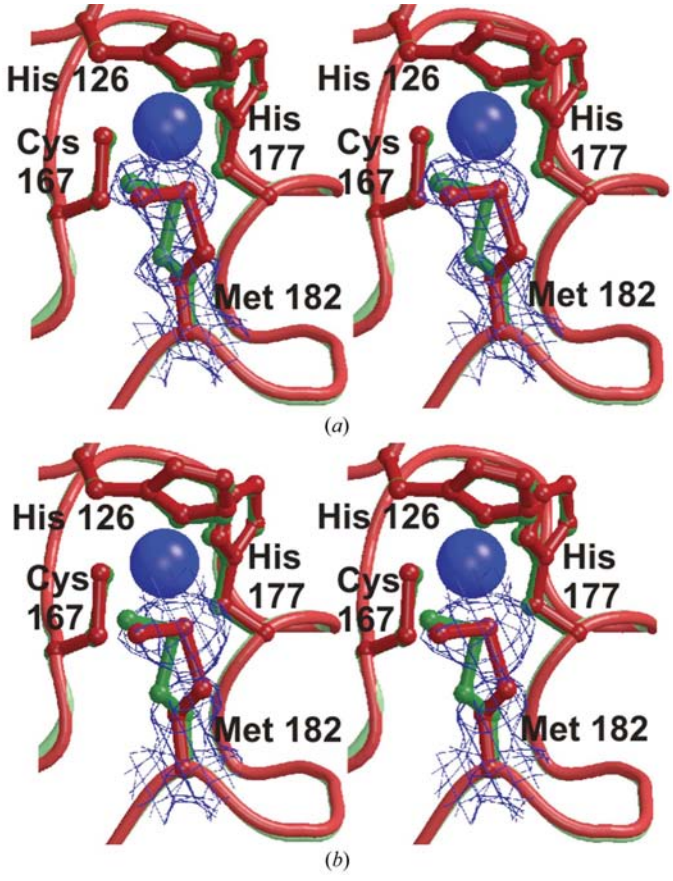

Figure 4
Stereoview of the type 1 Cu site showing electron density (omit map contoured at 1.2σ, blue netting) for (*a*) oxidized and (*b*) reduced Met182 in RsNiR. For comparison, both the refined structures of the oxidized (green) and reduced (red) structures are shown. (These figures were produced with *BOBSCRIPT*.)

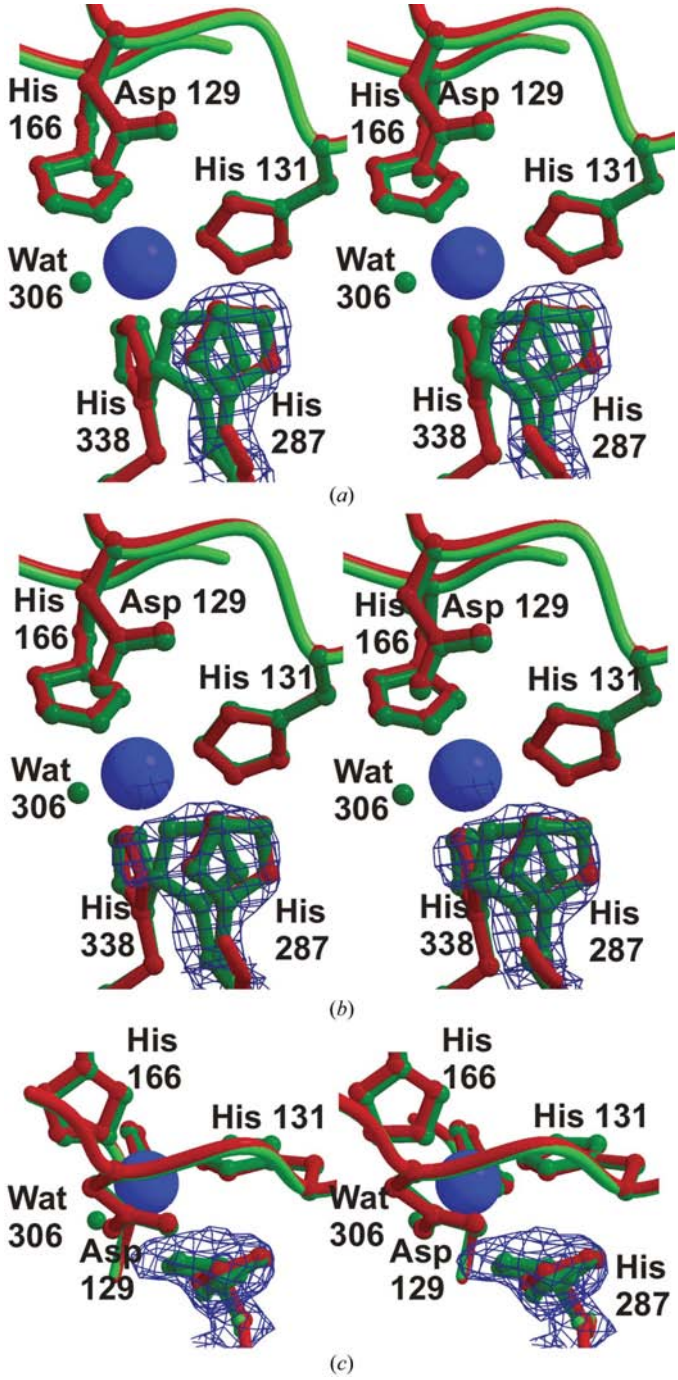

Figure 5
Stereoviews (side and top views) of the type 2 Cu site showing electron density on His287 ($2F_o - F_c$ omit map contoured at 1.0σ, blue netting) in the structures of reduced and oxidized RsNiR. For comparison, both the refined structures of the oxidized (green) and reduced (red) RsNiR are shown. In the oxidized structure, His287 is modelled with a dual conformation. (*a*) Electron density from the reduced structure (side view). (*b*) Electron density from the oxidized structure (side view). (*c*) Electron density from the oxidized structure (top view). (These figures were produced with *BOBSCRIPT*.)

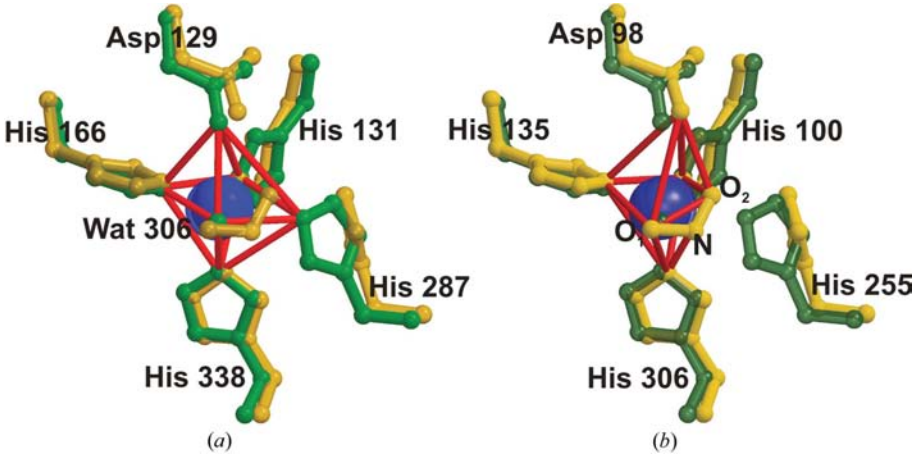

Figure 6
Pseudo-octahedral geometry of the type 2 Cu site. Structural models for both the oxidized RsNiR with the close conformation of His287 (green) and oxidized AfNiR with bound nitrite (yellow; PDB code 1as6) are overlaid. In (*a*) red lines are used to illustrate the distorted octahedral geometry of the oxidized RsNiR interaction sphere, whereas in (*b*) the same representation is used to illustrate the distorted octahedral geometry of the oxidized AfNiR with bound nitrite. (This figure was produced with *MOLSCRIPT*.)

context: two nitrite O atoms and three histidine N atoms (from His131, His166 and His338). Pentacoordinated copper in proteins can also be seen in azurin (Sykes, 1991) and although hexacoordinated copper is unusual in proteins, it exists more commonly in inorganic complexes.

The type 2 Cu site of NiR is usually considered to be tetracoordinated in the oxidized enzyme. If one considers the interactions of the Cu with both ligands and the catalytic residues, however, then this Cu site can be viewed as having five or six interactions depending on pH. Specifically, for the oxidized enzyme at high pH, Asp129 and His287 (in its close conformation; Fig. 6) together with the three histidine ligands (His131, His166 and His338) and the ligating water (Wat306) create a pseudo-octahedral geometry for the copper site with Asp129 and His338 as the axial residues (Table 4). Asp129 is somewhat distant (3.3 Å removed from the type 2 Cu) and is placed axially from His338 and completes a distorted octahedral geometry (Fig. 6*a*). Furthermore, when Asp was mutated to Glu in AxNiR (Ellis *et al.*, 2003), the lengthened side chain of the carboxyl group enabled it to ligate the Cu ion at a distance of 2.2 Å, thereby indicating that Asp129 strives to coordinate the copper. Asp129 forms a hydrogen bond to the ligating water (Wat306) without substrate present and forms a hydrogen bond to a nitrite O atom in the nitrite-soaked oxidized AfNiR structure (Fig. 6*b*). Since Asp129 is unlikely to be protonated at active pH, nitrite must be protonated in order to form a hydrogen bond to Asp129. The ligand field of the reduced type 2 Cu centre is tetrahedral, with a distorted pyramidal geometry, as has been seen in a previous reduced Cu-NiR structure (Murphy *et al.*, 1997). In summary, the oxidized type 2 Cu centre may be regarded as having octahedral interaction properties, while the reduced type 2 Cu centre has tetrahedral interaction properties.

Our observation that His287 adopts a close conformation to the type 2 Cu when it is deprotonated has implications for the mechanism of nitrite reduction at this site. Comparison of our structure (green, Fig. 6) with that of nitrite-soaked oxidized AfNiR (yellow; Fig. 6) shows that both structures share a distorted octahedral geometry. In this case, one O atom of the bound nitrite is at almost the same position as the water ligand (Wat306) and the second O atom of bound nitrite is at a position that would mean a steric clash with the N^{ε} of the His287 in the close conformation (Fig. 6). This result implies that when the pH is such that His287 is deprotonated, its N^{ε} atom competes for the position reserved for an O atom of nitrite and the interaction sphere of the type 2 Cu is completely filled. Thus, the energy cost of displacing both the ligating water and N^{ε} of His 287 is presumably unfavourable and nitrite is unable to bind at high pH. Indeed, preliminary results from the X-ray structure of RsNiR co-crystallized with a 50-fold excess of nitrite under the same conditions showed no evidence for bound nitrite. Furthermore, the activity of nitrite reductase drops rapidly above pH 6–7 (Abraham *et al.*, 1997) and it has been suggested that His287 must be protonated for the protein to be active (Adman *et al.*, 1995). Our observations provide a plausible structural explanation for these findings, since His287 will not compete with bound nitrite when it is protonated (*i.e.* at active pH). Likewise, it has been noted that the affinity of nitrite for the type 2 Cu site is lowered upon reduction (Murphy *et al.*, 1997). Our findings help to understand this phenomenon, since the two structures (oxidized and reduced RsNiR) recovered under otherwise identical crystallization conditions clearly agree with the theoretical fact that a distorted octahedral geometry of the type 2 Cu site is favourable for Cu^{2+}, but cannot form for Cu^{+}. Since nitrite binds to complete a distorted octahedral geometry (Fig. 6*b*), the specific ligating properties of the two redox states of the type 2 Cu ion could be the primary cause for the different binding affinities of nitrite.

We wish to thank the staff at beamline I711 of MaxLab for experimental support and Itai Panas and Örjan Hansson for helpful discussions. Financial support from the Swedish Research Council (VR), the Swedish Strategic Research Foundation (SSF) and SWEGENE are gratefully acknowledged. Finally, we acknowledge J. Shapleigh for introducing this project to KO.

References

Abraham, Z. H. L., Lowe, D. J. & Smith, B. E. (1993). *Biochem. J.* **296**, 885–885.
Abraham, Z. H. L., Smith, B. E., Howes, B. D., Lowe, D. J. & Eady, R. R. (1997). *Biochem. J.* **324**, 511–516.
Adman, E. T., Godden, J. W. & Turley, S. (1995). *J. Biol. Chem.* **270**, 27458–27474.

Basumallick, L., Szilagyi, R. K., Zhao, Y. W., Shapleigh, J. P., Scholes, C. P. & Solomon, E. I. (2003). *J. Am. Chem. Soc.* **125**, 14784–14792.
Boulanger, M. J., Kukimoto, M., Nishiyama, M., Horinouchi, S. & Murphy, M. E. P. (2000). *J. Biol. Chem.* **275**, 23957–23964.
Boulanger, M. J. & Murphy, M. E. P. (2002). *J. Mol. Biol.* **315**, 1111–1127.
Brünger, A. T., Adams, P. D., Clore, G. M., DeLano, W. L., Gros, P., Grosse-Kunstleve, R. W., Jiang, J.-S., Kuszewski, J., Nilges, M., Pannu, N. S., Read, R. J., Rice, L. M., Simonson, T. & Warren, G. L. (1998). *Acta Cryst.* D**54**, 905–921.
Chakrabarti, P. (1989). *Biochemistry*, **28**, 6081–6085.
Dodd, F. E., Hasnain, S. S., Abraham, Z. H. L., Eady, R. R. & Smith, B. E. (1997). *Acta Cryst.* D**53**, 406–418.
Dodd, F. E., Van Beeumen, J., Eady, R. R. & Hasnain, S. S. (1998). *J. Mol. Biol.* **282**, 369–382.
Ellis, M. J., Dodd, F. E., Sawers, G., Eady, R. R. & Hasnain, S. S. (2003). *J. Mol. Biol.* **328**, 429–438.
Ellis, M. J., Dodd, F. E., Strange, R. W., Prudencio, M., Sawers, G., Eady, R. R. & Hasnain, S. S. (2001). *Acta Cryst.* D**57**, 1110–1118.
Farver, O., Eady, R. R., Sawers, G., Prudencio, M. & Pecht, I. (2004). *FEBS Lett.* **561**, 173–176.
Fee, J. A. (1975). *Struct. Bonding*, **23**, 1–60.
Fülöp, V., Moir, J. W. B., Ferguson, S. J. & Hajdu, J. (1995). *Cell*, **81**, 369–377.
Howes, B. D., Abraham, Z. H. L., Lowe, D. J., Bruser, T., Eady, R. R. & Smith, B. E. (1994). *Biochemistry*, **33**, 3171–3177.
Inoue, T., Gotowda, M., Deligeer, Kataoka, K., Yamaguchi, K., Suzuki, S., Watanabe, H., Gohow, M. & Kai, Y. (1998). *J. Biochem. (Tokyo)*, **124**, 876–879.
Jones, T. A., Zou, J. Y., Cowan, S. W. & Kjeldgaard, M. (1991). *Acta Cryst.* A**47**, 110–119.
Kukimoto, M., Nishiyama, M., Murphy, M. E. P., Turley, S., Adman, E. T., Horinouchi, S. & Beppu, T. (1994). *Biochemistry*, **33**, 5246–5252.
Lamzin, V. S. & Wilson, K. S. (1993). *Acta Cryst.* D**49**, 129–147.
Laskowski, R. A., MacArthur, M. W., Moss, D. S. & Thornton, J. M. (1993). *J. Appl. Cryst.* **26**, 283–291.
Libby, E. & Averill, B. A. (1992). *Biochem. Biophys. Res. Commun.* **187**, 1529–1535.
Murphy, M. E. P., Turley, S. & Adman, E. T. (1997). *J. Biol. Chem.* **272**, 28455–28460.
Navaza, J. (1994). *Acta Cryst.* A**50**, 157–163.
Nurizzo, D., Silvestrini, M. C., Mathieu, M., Cutruzzola, F., Bourgeois, D., Fulop, V., Hajdu, J., Brunori, M., Tegoni, M. & Cambillau, C. (1997). *Structure*, **5**, 1157–1171.
Olesen, K., Veselov, A., Zhao, Y. W., Wang, Y. S., Danner, B., Scholes, C. P. & Shapleigh, J. P. (1998). *Biochemistry*, **37**, 6086–6094.
Otwinowski, Z. & Minor, W. (1997). *Methods Enzymol.* **276**, 307–326.
Pierloot, K., De Kerpel, J. O. A., Ryde, U., Olsson, M. H. M. & Roos, B. O. (1998). *J. Am. Chem. Soc.* **120**, 13156–13166.
Ryde, U., Olsson, M. H. M., Roos, B. O., De Kerpel, J. O. A. & Pierloot, K. (2000). *J. Biol. Inorg. Chem.* **5**, 565–574.
Sjogren, T. & Hajdu, J. (2001). *J. Biol. Chem.* **276**, 29450–29455.
Strange, R. W., Murphy, L. M., Dodd, F. E., Abraham, Z. H. L., Eady, R. R., Smith, B. E. & Hasnain, S. S. (1999). *J. Mol. Biol.* **287**, 1001–1009.
Suzuki, S., Kataoka, K., Yamaguchi, K., Inoue, T. & Kai, Y. (1999). *Coord. Chem. Rev.* **192**, 245–265.
Sykes, A. G. (1991). *Struct. Bonding*, **75**, 175–224.
Tocheva, E. I., Rosell, F. I., Mauk, A. G. & Murphy, M. E. P. (2004). *Science*, **304**, 867–870.
Tosques, I. E., Kwiatkowski, A. V., Shi, J. R. & Shapleigh, J. P. (1997). *J. Bacteriol.* **179**, 1090–1095.
Wijma, H. J., Boulanger, M. J., Molon, A., Fittipaldi, M., Huber, M., Murphy, M. E. P., Verbeet, M. P. & Canters, G. W. (2003). *Biochemistry*, **42**, 4075–4083.
Zumft, W. G. (1997). *Microbiol. Mol. Biol. Rev.* **61**, 533–616.